DOI: 10.1002/cbic.200800482

# Reversible Control of *Exo*- and *Endo*-Budding Transitions in a Photosensitive Lipid Membrane

Ken-ichi Ishii,[a] Tsutomu Hamada,*[a] Masaomi Hatakeyama,[b] Ryoko Sugimoto,[a] Takeshi Nagasaki,[c] and Masahiro Takagi[a]

*We have developed a method for the photomanipulation of lipid membrane morphology in which the shape of a vesicle can be switched by light through the use of a synthetic photosensitive amphiphile containing an azobenzene unit (KAON12). We prepared cell-sized liposomes from KAON12 and 1,2-dioleoyl-*sn*-glycero-3-phosphocholine (DOPC) and conducted real-time observations of vesicular transformation in the photosensitive liposome by phase-contrast microscopy. Budding transitions—either budding toward the centre of the liposome (*endo*-bud) or budding out of the liposome (*exo*-bud)—could be controlled by light. We discuss the mechanism of this transformation in terms of the change in the effective membrane surface area due to photoisomerization of the constituent molecules.*

## Introduction

Living cells and cellular organelles, such as the nucleus, the mitochondrion, the Golgi apparatus and endoplasmic reticulum, are commonly enclosed by a membrane with a lipid bilayer structure.[1] Cells actively change their structures in response to changes in the environment, such as chemical signals and/or physical conditions. Regulation of the lipid membrane structure is critical for many cellular processes, such as the budding–fission–fusion sequence of vesicular transport from the endoplasmic reticulum to the plasma membrane and the uptake of macromolecular aggregates through coated pits or phagocytosis.[2,3] The mechanical properties of the bilayer itself and/or embedded and associated proteins should play important roles in controlling these shapes.[4]

Recently, cell-sized liposomes ($>10\ \mu m$) have been actively studied as cell models, due to their similarities to natural cell structures in terms of size and membrane composition.[5] Since they are large enough to allow direct microscopic observation of the membrane behaviour of individual vesicles, investigations have been carried out on morphological dynamics in response to various internal and external stimuli (e.g., temperature,[6] chemical reaction inside or outside,[7] polymerization of encapsulated cytoskeleton,[8] addition of lanthanoid,[9] osmotic stress[10,11] and magnetic fluid load).[12] The development of methods to control the vesicular morphology could help us better understand the physicochemical properties of membrane structures and manipulate them as microreactors.[13,14] Along these lines, we have developed a photomanipulation method to control lipid vesicular shapes.[15] Light is an efficient experimental tool, because energy can be supplied without contact and without changing the chemical composition of the medium. In these experiments, the shape of an assembled vesicle could be switched through the action of a photosensitive amphiphilic molecule. Photoisomerization induced a change in membrane fluctuation behaviour or a morphological transition between ellipsoid and bud shapes. Although measurement of surface pressure versus area ($\pi$–*A*) curves implied that membrane area expansion is one of the possible factors in the shape changes, the detailed mechanism was not fully understood.

In the work reported in this paper we developed microscopic observations and found various novel budding phenomena—such as *exo*- and *endo*-budding transitions—that could be controlled reversibly. The photoinduced change in membrane area was directly measured by using the micropipette aspiration technique. We discuss the mechanism of these photoinduced transformations by comparing them with the changes in morphology observed in an osmotic shock experiment.

## Results and Discussion

Scheme 1 shows the chemical structure of KAON12,[16] a photoresponsive cationic lipid. The azobenzene component serves as the photoresponsive region, because UV induces marked structural and dipolar changes. KAON12 also contains lysine residues (basic hydrophilic groups) and a didodecylamide

[a] *K.-i. Ishii, Dr. T. Hamada, R. Sugimoto, Prof. M. Takagi*
*School of Materials Science, Japan*
*Advanced Institute of Science and Technology*
*1–1 Asahidai, Nomi, Ishikawa 923-1292 (Japan)*
*Fax: (+81) 761-51-1525*
*E-mail: t-hamada@jaist.ac.jp*

[b] *Dr. M. Hatakeyama*
*School of Knowledge Science, Japan*
*Advanced Institute of Science and Technology*
*1–1 Asahidai, Nomi, Ishikawa 923-1292 (Japan)*

[c] *Prof. T. Nagasaki*
*Graduate School of Engineering, Osaka City University*
*3-3-138 Sugimoto, Sumiyoshi-ku, Osaka 558-8585 (Japan)*

*Supporting information for this article is available on the WWW under http://dx.doi.org/10.1002/cbic.200800482.*

  

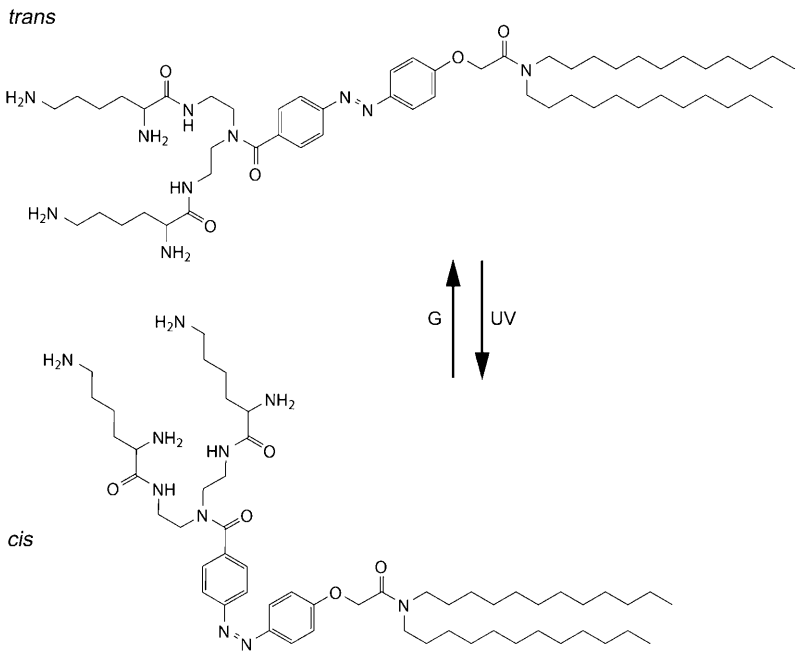


**Scheme 1.** KAON12. In our experiments, UV (365 nm) and green (G) light (546 nm) irradiation is used for isomerization.

structure (hydrophobic region). The photoisomerization between the *trans* and *cis* forms is reversible.

### Membrane fluctuation transitions upon photoisomerization

Figure 1 shows the effect of photoirradiation on a spherical liposome composed of a phospholipid, 1,2-dioleoyl-*sn*-glycero-3-phosphocholine (DOPC) and KAON12. Phase-contrast microscopy images of liposomes containing the *trans* or *cis* form of KAON12 with different fluctuation behaviour are shown in Figure 1 A. Initially, the liposome with a *trans* conformation shows a complete sphere without agitation. UV treatment to give *cis* isomerization enhances membrane undulation, and the recovery from *cis* to *trans* under green light suppresses this fluctuation. To clarify the difference in fluctuation behaviour between isomers, the change in the radius was measured (Figure 1 B). The radii were calculated as follows: 1) The edge of the liposome was extracted from the image data. 2) The centroid position from the edge was calculated. 3) The distances from the centroid to the outer edge for every $\pi/50$ radians were calculated. 4) The distance data were presented as a function of the angle. As shown in Figure 1 B, photoisomerization induced a marked change in membrane fluctuation, indicating that a vesicle with a *cis* form of KAON12 has surplus membrane area to encapsulate the inner aqueous solution (that is, a large enough ratio of membrane area to an enclosed volume). Such large vesicular fluctuation requires membrane excess area.[17] In contrast, little fluctuation in the periphery of the *trans* form of KAON12 suggests that the membrane area fits the spherical surface of the inner liquid phase.

It is known that the membrane fluctuation of quasispherical vesicles can be analysed by Fourier decomposition.[18] The amplitudes of membrane fluctuation corresponding to Figure 1 B were calculated as a function of angular frequency, $q$ (Figure 1 C). The Fourier decomposition of the function $r(\theta,t)$ was calculated to obtain the Fourier coefficients $a_q(t)$ and $b_q(t)$. Amplitude was defined as $(a_q^2+b_q^2)^{1/2}$. In this snapshot, the second periodical element ($q=2$, ellipticity), is the greatest, followed by the third element ($q=3$, asymmetry).[7,19] The clean $q=2$ peak shows typical ellipsoidal fluctuation. To confirm the dynamics of fluctuation, the amplitudes of the second and third periodical elements are calculated as a function of time in Figure 2. The results indicate that the spherical vesicle fluctuates after UV treatment and that the second element is greater than the third, on average, during *cis* isomerization. Such $q$ dependency in fluctuation behaviour is in agree-

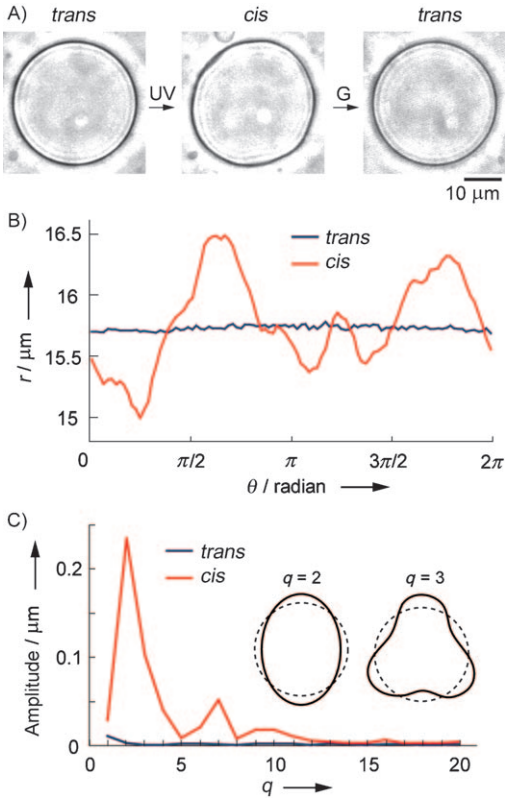


**Figure 1.** A) Phase-contrast microscopy images of the different fluctuation behaviour of *trans*- and *cis*-form liposomes. B) Spatial fluctuation in the radius ($r$) around the contour. C) Amplitude versus frequency ($q$) of membrane fluctuation, as obtained by Fourier analysis.

  

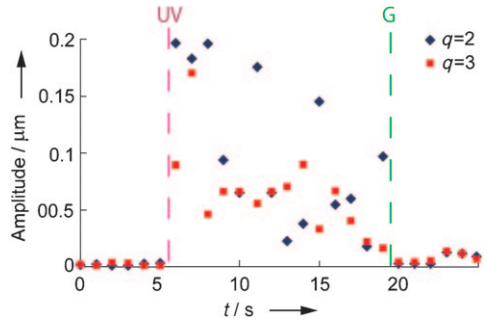


**Figure 2.** Amplitude versus time for frequency $q=2$ and $q=3$ in membrane fluctuation under photoirradiation.

ment with the fluctuation spectrum calculated from the equipartition theorem reported elsewhere.[19]

### Reversible control of membrane budding transitions

Figure 3 A shows the dynamic response of a liposome with an endocytic daughter vesicle to photoisomerization. Previous experiments on the swelling of lipid films have shown that such deformed liposomes are generated rather frequently together with their spherical counterparts.[5] An *endo*-bud liposome is thus obtained independently of any specific experimental procedure. From careful observation of the Brownian motion of the daughter vesicle, we consider that the daughter vesicle is not separate, but rather is connected to the mother liposome. As shown in Figure 3 A, under UV light the liposome started to undulate and then took in the small inner vesicles. The strongly fluctuating membrane expelled a small bud outside. The position of the daughter vesicle thus shifted from inside to outside the mother liposome. Interestingly, under green irradiation, we observed that part of the liposome invaginated and satellite vesicles budded toward the centre of the mother liposome (i.e., the liposome again had endocytic daughter vesicles). Figure 3 B shows the time-dependent change in the diameter of the mother liposome. The "birth" of an exocytic vesicle under UV light led to a decrease in liposome diameter, while an increase in liposome diameter was seen with the formation of an endocytic vesicle. This volume difference can be explained in terms of the continuity of the whole membrane area. Since the interiors of the daughter vesicles are connected to the bulk solution, the volume of the mother liposome with an *endo*-bud (*trans*) is just that much greater than the vesicular volume with an *exo*-bud (*cis*). Although the pathway for transformation varies somewhat between the forward and reverse processes, the transition between two stable states—that is, inner- and outer-attached satellite vesicles—is reversible.

Figures 4 and 5 show the results of photoirradiation of liposomes of various shapes that are also spontaneously formed through natural swelling of the lipid film. We found that these liposomes exhibit unique shape changes. Figure 4 A shows a prolate–bud transition. After UV irradiation, the prolate vesicle exhibits budding. The two spherical buds are connected by a small neck. Moreover, the budding vesicle transforms back into the original prolate shape upon treatment with green light.

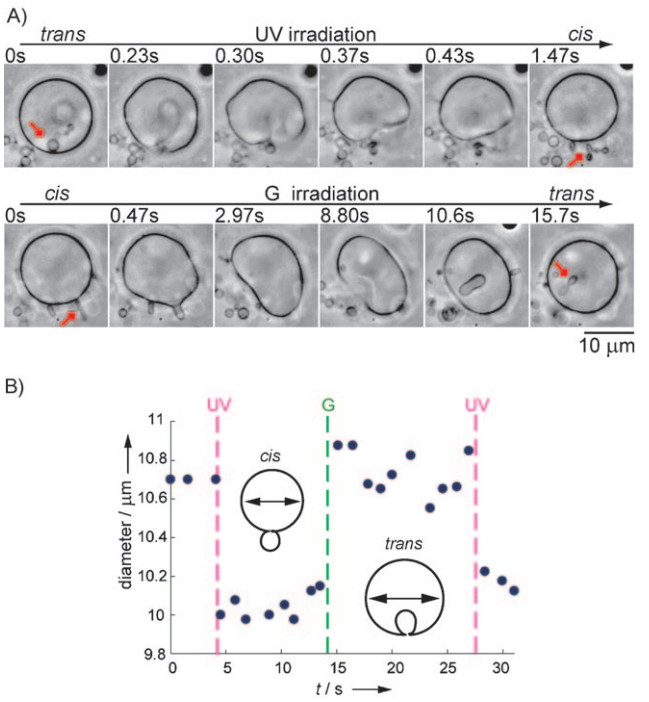


**Figure 3.** Photoinduced reversible vesicular transport across a bilayer membrane. A) Phase-contrast photomicrographs. Time elapsed after UV or green (G) irradiation. B) Time-dependent change in the diameter of the mother liposome.

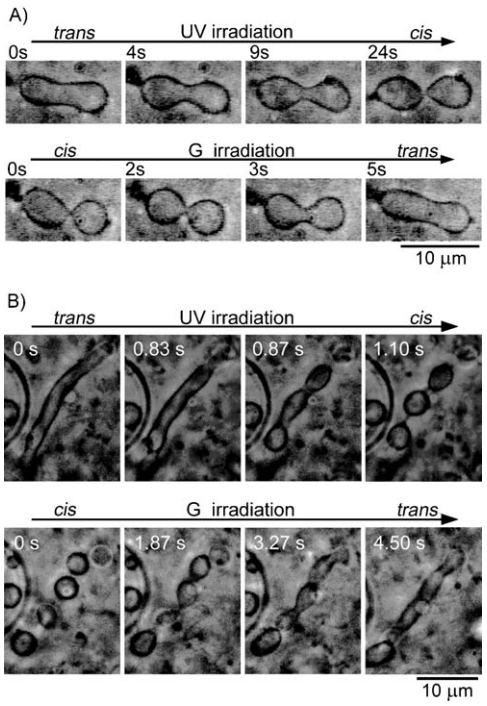


**Figure 4.** Photoinduced reversible budding transitions. A) Prolate–bud transition. B) Tubular–necklace transition. Transformation from prolate/tubular to bud/necklace induced by UV light. Reverse process from bud/necklace to prolate/tubular induced by irradiation with green light. Time elapsed after UV or green irradiation.

  

Next, we focused on a tubular—that is, elongated prolate—shape and observed a reversible tubular–necklace transition (Figure 4B). Under UV irradiation, the tubular liposome developed a necklace shape (that is, a number of spherical vesicles connected by narrow necks). The necklace liposome then transformed back into the tubular shape under green light.

Figure 5 shows the stomatocyte (*trans*)–bud (*cis*) transition. The stomatocyte liposome has a stable invaginated part, like a morphologically abnormal erythrocyte. UV irradiation destabilized this morphology and induced the budding transition. The obtained *exo*-bud liposome has two spherical vesicles connected by a small neck. We can also control the reverse transformation, *exo*-bud to stomatocyte, by using green light. In response to isomerization from the *trans*-azo to *cis*-azo form, all asymmetrical liposomes (Figures 4 and 5) underwent the same budding profile as the vesicular transportation shown in Figure 3: the membrane with a *cis*-azo form tends to have an *exo*-bud shape. Notably, we have never observed the separation of budded vesicles under these experimental conditions. We confirmed that even prolonged (several minutes) photoirradiation cannot induce a break in the narrow neck between vesicles, indicating that additional forces are needed to create two new vesicles from the initial one.

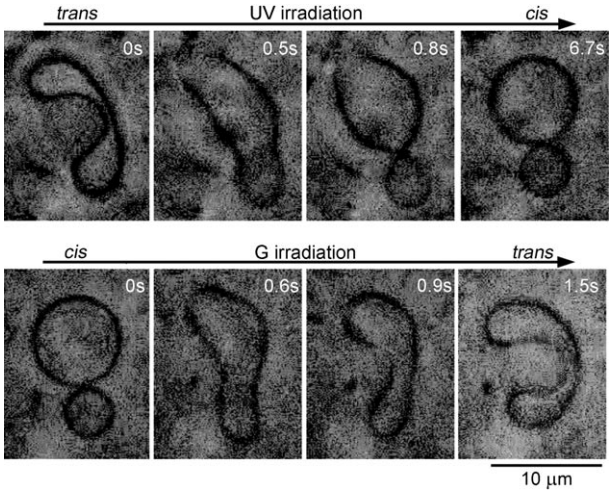


**Figure 5.** Photoinduced reversible stomatocyte–bud transition. Transformation from stomatocyte to exo-bud induced by UV light. Reverse process from exo-bud to stomatocyte induced by irradiation with green light. Time elapsed after UV or green irradiation.

### The change in the membrane excess area determines the stable transition morphologies

We found that photoisomerization induces several membrane-budding phenomena, such as *endo*-bud (*trans*) and *exo*-bud (*cis*) in Figure 3, prolate (*trans*) and *exo*-bud (*cis*) in Figure 4, and stomatocyte (*trans*) and *exo*-bud (*cis*) in Figure 5. The photoinduced transformations can be attributed to changes in membrane surface area. We know from our experiments on $\pi$–*A* curves of a Langmuir monolayer that the surface area per molecule in the *cis*-azo form is greater than that in the *trans*-azo form at the same pressure.[15] The enhanced membrane fluctuation of the quasispherical liposome with a *cis*-azo form in Figure 1 also confirmed this scenario. Notably, the volume change is negligible relative to the photoinduced change in surface area on the timescale of our observation; this is due to the low permeability of water through a phospholipid bilayer membrane. To characterize the photoeffect on the bilayer membranes, we measured the change in membrane area upon photoirradiation by a micromanipulation technique (see the Supporting Information).[20] Figure 6 shows the distribution of area expansion ratio in the photosensitive liposomes. The average ratio of the area expansion was $3.2 \pm 1.6$%. The dispersion is probably the result of wide variation in the mixed fraction of KAON12 during the liposome preparation.

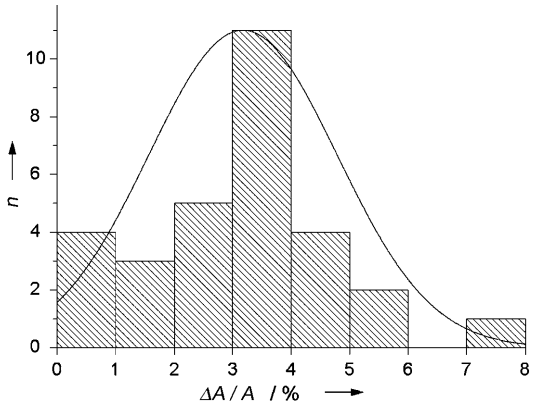


**Figure 6.** Distribution of membrane area expansion upon photoirradiation. The solid line is a Gaussian fit to the data.

To facilitate better understanding of these photoinduced morphological transitions in terms of changes in membrane area, we investigated the behaviour of the membrane morphology under osmotic stress. When the liposomes are subjected to high osmolarity, the water efflux across the membranes reduces the inner aqueous volume, indicating that the liposomes acquire excess surface area.[8] The excess area is a parameter that describes the membrane morphology in terms of Helfrich bending energy,[21] which is defined by the ratio of area to volume and is also called the reduced volume.[22] In this context, the change in the interior volume with constant area produced by osmosis is comparable to the change in area with constant volume produced by photoisomerization. Figure 7 shows the typical evolution of liposome morphology as the result of a gradual increase in the membrane excess area due to osmotic pressure.[23] After osmotic pressure was applied, a thin, flexible filament, most probably attached to the mother liposome, was observed in the vesicular space (Figure 7B). The daughter filament gradually thickened (i.e., a tubular structure with a micron-sized internal core; Figure 7C). As shown in Figure 7D, the tube then became shorter and thicker, with a similar morphology to the *endo*-bud liposome in Figure 3A. Interestingly, the contact point between the inner vesi-

  

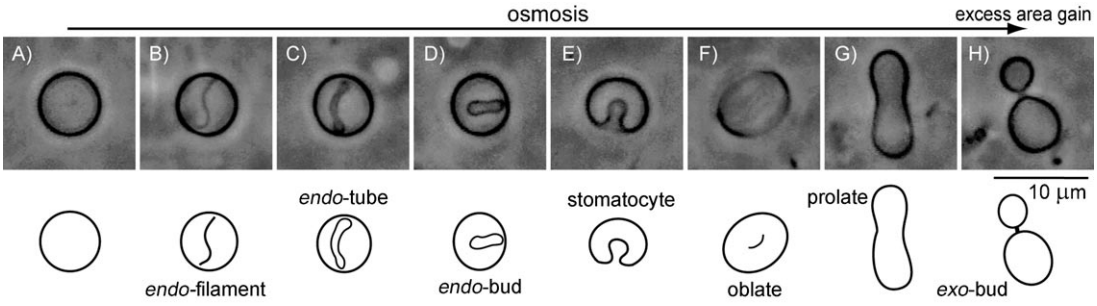


**Figure 7.** Transformation pathway in response to osmotic stress, together with schematic illustrations. The osmotic environment is $\Delta c = 0.5$ mM glucose solution. Elapsed times are A) 125, B) 436, C) 914, D) 968, E) 1033, F) 1058, G) 1103, and H) 1118 s.

cle and the outer membrane started to open and the shape of the liposome changed into the stomatocyte form (Figure 7E). After the invaginated area was completely opened, the liposome acquired an oblate shape (Figure 7F). Finally, the oblate liposome elongated until it was prolate (Figure 7G), and an *exo*-bud formed (Figure 7H). This change in morphology—from an *endo*-bud to an *exo*-bud through stomatocyte, oblate and prolate—thus occurs with an increase in excess area. These shapes are expected to have a minimum membrane bending energy for each excess area,[24] so the energetically stable shape shifted with changes in the membrane excess area due to osmotic stress.

The vesicular shapes observed in the osmotic evolution (Figure 7) are consistent with the photoinduced morphological transitions (Figures 3, 4 and 5). The initial morphologies before photoirradiation are determined by the process of liposome formation; during hydration, liposomes with different water volumes—that is, different excess areas–-are formed, which leads to various asymmetric morphologies. In the case of endo- and exocytic vesiculation as shown in Figure 3, the *endo*-bud (*trans*) and exo-bud (*cis*) correspond to the morphologies in Figure 7D and 7H, respectively, in the osmotic pathway. For the transition between prolate (*trans*) and exo-bud (*cis*) in Figure 4A, the prolate shape was observed in Figure 7G and a bud was seen in Figure 7H. The stomatocyte (*trans*) vesicle in Figure 5 was similar to that in Figure 7E. Moreover, the entire course of transformation upon photoisomerization from *trans* to *cis*—that is, with excess area gain—is consistent with the changes due to osmotic stress; this reveals that the change in excess area due to isomerization is essential for the morphological transitions. The ratio of membrane area expansion deduced from the excess area gain in the osmotically induced transformation from *endo*-bud into exo-bud is $\Delta A/A = 3.6\%$ (see the Supporting Information), which is in good agreement with the result ($3.2 \pm 1.6\%$) from the micropipette aspiration measurements. Notably, although we showed typical light-induced vesicular transformations in Figures 3, 4 and 5, liposomes with similar initial shapes did not always show uniform transformations. A stomatocyte liposome, for example, can transform into a prolate shape. This variation results from a difference in the excess area changed by photoisomerization (Figure 6), since there has to be some dispersion in the mixing ratio of KAON12 over the liposomes obtained through the gentle hydration method. The reversibility of the shape transitions was very high ($>90\%$).

When photoresponsive liposomes were used in a gene delivery experiment, it was reported that the transfection efficiency achieved with KAON12 was higher than that obtained with Lipofectin, a commercially available lipid gene carrier.[16] Once the KAON12/DNA complex has passed through the plasma membrane by endocytosis, *trans*-to-*cis* isomerization of the azobenzene moiety would destabilize the liposome membrane, thus accelerating the membrane fusion of photoresponsive liposomes with cellular organelles. These results imply that the azo-lipid might induce not only the described morphological transitions in the shape of a single vesicle, but also changes in membrane topology between neighbouring membranes. As a future research target, it might useful to try to control the fusion of lipid membranes by use of light-sensitive giant liposomes for the design of better lipid gene carriers and for use as microreactors.[25]

## Conclusions

We have conducted real-time observations of vesicular transformations in liposomes with an azo-lipid under photoirradiation conditions. The results clearly demonstrate that the liposome exhibited various reversible transitions, such as *exo*- and *endo*-budding, due to photoisomerization of the constituent molecule. Because the photoinduced shape transitions agreed well with the morphological changes that occurred due to increases in excess area caused by osmotic pressure, the mechanism of these photoinduced transformations is interpreted in terms of changes in membrane surface area. Very recently, photocontrol of DNA conformation with the aid of an azo-surfactant has been reported.[26] The light-induced encapsulation of macromolecules with an azo-polymer was also presented.[27] Photons are potent stimuli that can be used for timing-specific control of biological macromolecules. These findings may provide insight into the biophysics of membrane mechanics and a basis for their wide practical applications together with photoirradiation.

  

## Experimental Section

**Materials**: We designed and synthesized a photosensitive amphiphilic molecule containing azobenzene (KAON12); the conformation (*trans* or *cis*) of this molecule can be switched by light irradiation (Scheme 1). 1,2-Dioleoyl-*sn*-glycero-3-phosphocholine (DOPC) was purchased from Avanti Polar Lipids (Alabaster, USA). Deionized water obtained from a Millipore Milli Q purification system was used to prepare reagents.

**Preparation of photosensitive cell-sized liposomes**: Liposomes were prepared by the natural swelling method from dry lipid films; lipid mixtures (KAON12 and DOPC) dissolved in methanol/chloroform (1:2, *v/v*) in a glass test tube were dried under vacuum for 2 h to form thin lipid films. The films were then hydrated overnight with deionized water at 37 °C. The final concentration was 0.5 mM of lipids (KAON12/DOPC 3:4).[28] Using a conventional microscopic method with fluorescent dyes to monitor lipid segregations within bilayer membranes,[11] we confirmed that no segregation on the KAON12/DOPC membrane surface was detectable.

**Microscopic observation under photoirradiation conditions**: The liposome solution (5 μL) was placed on a glass coverslip, which was covered with another smaller coverslip at a spacing of ca. 0.2 mm. We observed changes in membrane morphology with a phase-contrast microscope (Olympus BX50, Japan) at room temperature and irradiated membranes through standard filter sets, (WU, Olympus; $\lambda_{ex}$ = 330–385 nm, dichroic mirror 400 nm, $\lambda_{em}$ = 420 nm and WIG, Olympus; $\lambda_{ex}$ = 520–550 nm, dichroic mirror 565 nm, $\lambda_{em}$ = 580 nm), with use of an extra-high-pressure mercury lamp (100 W) for photoisomerization. Irradiation time was less than a second (no effect of sample heating). The ratios of *trans*-/*cis*-azo under UV and green illumination are approximately 1:4 and 4:1, respectively.[15] The images were recorded on a hard-disc drive at 30 frames $s^{-1}$.

**Micropipette aspiration**: Liposomes (KAON12/DOPC 3:4) were prepared with sucrose solution (100 mM). An aliquot of the liposome solution (10 μL) was then mixed with glucose solution (100 mM, 290 μL). The difference in the refractive indices of the internal and external solutions enhances the image contrast of liposomes. A single liposome was aspirated into a glass micropipette (Eppendolf, CustomTip Type 1, inner diameter 10 μm). We used a micromanipulator (Narishige, MN-151) and a microinjector (Eppendorf, CellTram Vario), set on an inverted differential interference contrast (DIC) microscope (Nikon TE2000, Japan).

**Treatment with osmotic stress**: Liposome and glucose solution (1 mM) were poured into a test tube and gently mixed by soft tapping. The difference in the molar concentration of glucose across the bilayer membrane was 0.5 mM.

## *Acknowledgements*

*The authors thank S. Araki (Kyoto University) for valuable discussions, and K. Kawaguchi (JAIST) for his skilled technical assistance. This work was supported by a KAKENHI Grant-in-Aid for Scientific Research (B) (No. 20360370) from the Japan Society for the Promotion of Science (JSPS), and on Priority Areas "Soft Matter Physics", "Bio Manipulation" and "Life Surveyor" from the Ministry of Education, Culture, Sports, Science and Technology of Japan (MEXT). T.H. was supported by the Research for Promoting Technological Seeds program from the Japan Science and Technology Agency (JST) .*

**Keywords:** azobenzenes · budding · liposomes · membranes · photocontrol

[1] B. Alberts, A. Johnson, J. Lewis, M. Raff, K. Roberts, P. Walter in *Molecular Biology of the Cell*, 5th ed. Garland Science, New York, **2008**.
[2] H. T. McMahon, J. L. Gallop, *Nature* **2005**, *438*, 590–596.
[3] K. Trajkovic, C. Hsu, S. Chiantia, L. Rajendran, D. Wenzel, F. Wieland, P. Schwille, B. Brügger, M. Simons, *Science* **2008**, *319*, 1244–1247.
[4] R. Lipowsky, E. Sackmann in *Structure and Dynamics of Membranes, Vol. 1A*, Elsevier, Amsterdam, **1995**.
[5] P. L. Luisi, P. Walde in *Giant Vesicles Perspectives in Supramolecular Chemistry, Vol. 6*, Wiley, Chichester, **2000**.
[6] J. Käs, E. Sackmann, *Biophys. J.* **1991**, *60*, 825–844.
[7] P. G. Petrov, J. B. Lee, H.-G. Döbereiner, *Europhys. Lett.* **1999**, *48*, 435–441.
[8] H. Hotani, T. Inaba, F. Nomura, S. Takeda, K. Takiguchi, T. J. Itoh, T. Umeda, A. Ishijima, *BioSystems*, **2003**, *71*, 93–100.
[9] T. Tanaka, Y. Tamba, S. M. Masum, Y. Yamashita, M. Yamazaki, *Biochim. Biophys. Acta Biomembr.* **2002**, *1564*, 173–182.
[10] A. L. Bernard, M. A. Guedeau-Boudeville, L. Jullien, J. M. di Meglio, *Biochim. Biophys. Acta Biomembr.* **2002**, *1567*, 1–5.
[11] T. Hamada, Y. Miura, K. Ishii, S. Araki, K. Yoshikawa, M. Vestergaard, M. Takagi, *J. Phys. Chem. B* **2007**, *111*, 10853–10857.
[12] C. Ménager, D. Guemghar, R. Perzynski, S. Lesieur, V. Cabuil, *Langmuir* **2008**, *24*, 4968–4974.
[13] K. Sott, T. Lobovkina, L. Lizana, M. Tokarz, B. Bauer, Z. Konkoli, O. Orwar, *Nano Lett.* **2006**, *6*, 209–214.
[14] A. Tian, C. Johnson, W. Wang, T. Baumgart, *Phys. Rev. Lett.* **2007**, *98*, 208102.
[15] T. Hamada, Y. T. Sato, T. Nagasaki, K. Yoshikawa, *Langmuir* **2005**, *21*, 7626–7628.
[16] T. Nagasaki, S. Shinkai, *J. Incl. Phenom. Macrocycl. Chem.* **2007**, *58*, 205–219.
[17] T. Umeda, F. Nomura, T. Inaba, K. Takiguchi, H. Hotani, *ChemPhysChem* **2005**, *6*, 1047–1050.
[18] H. P. Duwe, E. Sackmann, *Physica A* **1990**, *163*, 410–428.
[19] V. Nikolov, R. Lipowsky, R. Dimova, *Biophys. J.* **2007**, *92*, 4356–4368.
[20] E. Evans, D. Needham, *J. Phys. Chem.* **1987**, *91*, 4219–4228.
[21] H. J. Deuling, W. Helfrich, *Biophys. J.* **1976**, *16*, 861–868.
[22] H. G. Döbereiner, *Curr. Opin. Colloid Interface Sci.* **2000**, *5*, 256–263.
[23] We also observed another transformation pathway (see the Supporting Information). After the application of an osmotic effect, some small vesicles appeared in the vesicular space, and these inner vesicles gradually grew bigger, as reported in ref. 10.
[24] U. Seifert, K. Berndl, R. Lipowsky, *Phys. Rev. A* **1991**, *44*, 1182–1202.
[25] W. Su, Y. Luo, Q. Yan, S. Wu, K. Han, Q. Zhang, Y. Gu, Y. Li, *Macromol. Rapid Commun.* **2007**, *28*, 1251–1256.
[26] M. Sollogoub, S. Guieu, M. Geoffroy, A. Yamada, A. Estévez-Torres, K. Yoshikawa, D. Baigl, *ChemBioChem* **2008**, *9*, 1201–1206.
[27] M. Bédard, A. G. Skirtach, G. B. Sukhorukov, *Macromol. Rapid Commun.* **2007**, *28*, 1517–1521.
[28] The photoswitching in vesicular shapes can be observed with above ~20% molar fraction of KAON12. We have previously reported the photoinduced effect with KAON12/DOPC 3:5 in ref. 15. No apparent difference in the photoinduced transitions was noted between the previous (3:5; ~38%) and current (3:4; ~43%) fractions of KAON12.

Received: July 15, 2008
Published online on January 8, 2009

  